

## Dynamical self-affinity of damage spreading in surface growth models

Yup Kim\* and C. K. Lee

*Department of Physics, Kyung-Hee University, Seoul 130-701, Korea  
and Asia Pacific Center for Theoretical Physics, Seoul, Korea*

(Received 8 May 2000)

The dynamical anisotropic scaling properties of the surface growth models are restudied by use of the damage spreading concept. For that the vertical damage spreading distance  $d_{\perp}$  of a damaged column as well as the lateral damage spreading distance  $d_{\parallel}$  is introduced. The scaling *Ansätze* for  $\bar{d}_{\perp}(d_{\parallel}, t)$ ,  $D_{\parallel} \equiv \langle d_{\parallel} \rangle$  and  $D_{\perp} \equiv \langle \bar{d}_{\perp} \rangle$  are suggested. The critical property of the probability distribution  $P(d_{\parallel}, t)$  for the survived damages is also suggested. The suggested scaling relations are tested by simulating various growth models with substrate dimension  $d=1$ . From these results it can be concluded that the critical property or dynamical self-affinity of a surface growth model can also be determined by investigating the damage spreading.

PACS number(s): 05.40.-a, 05.70.Ln, 68.35.Fx, 81.10.Aj

### I. INTRODUCTION

The application of the damage spreading (DS) concept to dynamical cooperative systems has been found to be a powerful tool for the investigation of the dynamical properties of the given systems [1]. For DSs two identical systems, which are initially the same, except for a small subset of the system, are simulated by the same random numbers and it is observed how damages are spreading during the dynamical evolution by a detailed comparison of the two systems. The method has been successfully applied to the analyses of some dynamical systems such as biological systems [2], cellular automata [3], kinetic Ising models [4–10], and spin glass systems [11]. Recently a study [12] has applied the DS concept to the kinetic surface roughening phenomena. This study has tried to relate initial damage spreading to the dynamical correlation of surface roughening phenomena.

The dynamical interface roughenings in the various growth models [13–21] have extensively been studied, because of the practical importance for material growths and the theoretical interest in the dynamical self-affine scaling property. The dynamical self-affine properties have mainly been analyzed by the surface width  $W(L, t)$ , which is defined by the root-mean-square fluctuation of the surface height. In many cases [13–21]  $W(L, t)$  has been known to satisfy the scaling *Ansatz*

$$W(L, t) = L^{\alpha} f(t/L^z), \quad (1)$$

where  $f(x) \approx x^{\beta}$  ( $\beta = \alpha/z$ ) for  $x \ll 1$  and  $f(x) \approx \text{const}$  for  $x \gg 1$ . Here  $L$  is the linear size of the substrate. It was found in Ref. [12] that  $D_0(t) \propto t^{1/z}$  when  $t \ll L^z$  for the growth models with  $\alpha < 1$ . Here  $D_0(t)$  was a lateral DS distance (or a DS distance parallel to the substrate). This result physically means that  $D_0$  can be related to the dynamical correlation length  $\xi$ , since  $\xi \approx t^{1/z}$  when  $t \ll L^z$  [13]. Although the study based on  $D_0(t)$  [12] partly explains the correlation dynamics, it cannot explain the dynamic self-affinity (or anisotropic scaling property) [13] of the roughening phenomena com-

pletely. In this paper we want to apply DS concepts to kinetic surface roughenings on a complete theoretical basis for the dynamical self-affinity. In order to do so a vertical damage spreading distance (or a DS distance perpendicular to the substrate) as well as a lateral distance must be introduced. The dynamical scaling relation of DSs which corresponds to Eq. (1) can be established by use of the two kinds of distances.

### II. SCALING RELATIONS FOR DAMAGE SPREADING

Now we explain the theoretical basis of our analysis for the DSs in the kinetic surface roughening phenomena. Consider two systems A and B of a growth. In system A growth begins with the flat surface, i.e.,  $h^A(r, 0) = 0$  for any  $r$  on the substrate. In contrast growth in system B begins with  $h^B(r, 0) = 0$  except at one point  $r_0$ , where  $h^B(r_0, 0) = 1$ . Here  $\{h^A(r, t)\}$  [ $\{h^B(r, t)\}$ ] means the surface height of system A [B] at  $t$ . The surfaces in A and B are allowed to grow under the same growth rule and under the same sequence of random numbers. A damaged column (or a damaged site) at  $t$  is defined by  $r$  at which  $h^A(r, t) \neq h^B(r, t)$ . If a column at  $r_d$  is damaged, then a lateral damage spreading distance  $d_{\parallel}$  and a vertical damage spreading distance  $d_{\perp}$  of the column are defined by

$$d_{\parallel} \equiv |r_d - r_0|, \quad d_{\perp} \equiv |h^B(r_d, t) - \langle h^B \rangle|, \quad (2)$$

where  $\langle h^B \rangle$  means the average surface height in system B. If the periodic boundary condition is imposed, then  $d_{\parallel}$  must satisfy  $d_{\parallel} \leq L/2$ . To study conventional dynamical systems such as Ising model through DS concepts, the main quantity or order parameter to focus on is the fraction of damaged sites or the Hamming distance [5]. In contrast we inevitably need the geometrical (real) distances to study kinetic surface roughening phenomena. Furthermore, to understand the intrinsic anisotropy or the self-affinity between the direction parallel to the substrate and the direction vertical to the substrate, lateral and vertical distances must simultaneously be considered.

To study the dynamical scaling property of surfaces by damage spreading the main relation to focus on is the rela-

\*Email address: ykim@nms.kyunghee.ac.kr

tion between  $d_{\perp}$  and  $d_{\parallel}$  or the function  $\bar{d}_{\perp}(d_{\parallel}, t)$ . Here  $\bar{d}_{\perp}(d_{\parallel}, t)$  means the average of  $d_{\perp}$  over the surviving damages which exist only at the lateral distance  $d_{\parallel}$  (or at  $r_d = r_0 \pm d_{\parallel}$ ). The function  $\bar{d}_{\perp}(d_{\parallel}, t)$  should have all the detailed information on damage spreading in the surface growth. We now want to suggest a reasonable scaling *Ansatz* for  $\bar{d}_{\perp}(d_{\parallel}, t)$ . In the early stage of growth it can be expected that damages should appear only at the columns near  $r_0$  if the spreading velocity is finite. So the touch time  $t_i(d_{\parallel})$  at which a damage first appears on the column at  $d_{\parallel}$  can be defined. Then for  $t < t_i(d_{\parallel})$  the damages have not spread to the column at  $d_{\parallel}$ , yet. For  $t > t_i(d_{\parallel})$  the damages have already spread over the column at  $d_{\parallel}$ . If DS faithfully describes the dynamical correlation of the surface growth, then the damage has spread over the columns at  $d_{\parallel} \leq \xi(t)$  [12]. Here  $\xi(t)$  means the correlation length of the surface roughening with  $\xi(t) \approx t^{1/z}$  [13]. It is thus reasonable to set  $t_i(d_{\parallel})$  as

$$t_i(d_{\parallel}) = cd_{\parallel}^z, \quad (3)$$

where  $c$  is a proportional constant. The reasonable scaling *Ansatz* for  $\bar{d}_{\perp}(d_{\parallel}, t)$  is then

$$\bar{d}_{\perp}(d_{\parallel}, t) \begin{cases} = 0 & \text{if } t - cd_{\parallel}^z < 0, \\ = A(t - cd_{\parallel}^z)^{\beta} & \text{if } 1 \ll t - cd_{\parallel}^z \ll L^z, \\ \approx L^{\alpha} & \text{if } t - cd_{\parallel}^z \gg L^z. \end{cases} \quad (4)$$

If  $t - cd_{\parallel}^z < 0$ , there is no damage in the column at  $d_{\parallel}$  and the first case in Eq. (4) is justified. If  $1 \ll t - cd_{\parallel}^z \ll L^z$ , at least a damage has already appeared in the column at  $d_{\parallel}$  and the vertical damage spreading should be in the initial stage. If the damage spreading in this regime can describe the early stage of the growth, i.e., the stage when  $W(L, t)$  satisfies  $W(L, t) \approx t^{\beta}$  [13], then the second case of Eq. (4) is justified. The fact that the time dependence is not like  $t^{\beta}$  but like  $(t - cd_{\parallel}^z)^{\beta}$  reflects the delayed start of vertical DS in the column at  $d_{\parallel} \neq 0$  by the amount of  $t_i (= cd_{\parallel}^z)$  compared to that at  $d_{\parallel} = 0$ . If  $t - cd_{\parallel}^z \gg L^z$ , then all growth is in the saturation regime of Eq. (1) [13]. The vertical DSs at all the columns in this regime should be saturated and thus the third case in Eq. (4) is also justified. The dynamical scaling form which summarizes all the cases in Eq. (4) should be

$$\bar{d}_{\perp} = L^{\alpha} f_{\perp} \left( \frac{t - cd_{\parallel}^z}{L^z} \right). \quad (5)$$

One more quantity which we consider important for the analysis of DS is the probability distribution of the survived damages at  $d_{\parallel}$ ,  $P(d_{\parallel}, t)$ . Of course  $P(d_{\parallel}, t) dd_{\parallel}$  is the probability to find a survived damage in the interval  $(d_{\parallel}, d_{\parallel} + dd_{\parallel})$ . If one knows  $P(d_{\parallel}, t)$ , the average lateral DS distance  $D_{\parallel}$  and average vertical DS distance  $D_{\perp}$  can be obtained from

$$D_{\parallel} = \langle d_{\parallel} \rangle = \int_0^{L/2} d_{\parallel} P(d_{\parallel}, t) dd_{\parallel} \quad (6)$$

and

$$D_{\perp} = \langle \bar{d}_{\perp} \rangle = \int_0^{L/2} \bar{d}_{\perp}(d_{\parallel}, t) P(d_{\parallel}, t) dd_{\parallel}. \quad (7)$$

Next we want to suggest a reasonable scaling *Ansatz* for  $D_{\parallel}$  and  $P(d_{\parallel}, t)$ . If the lateral damage spreading faithfully explains the lateral correlation dynamics of the surface growth phenomena,  $D_{\parallel}(L, t)$  should behave critically in the same way as the dynamical correlation length  $\xi$  [13] and the plausible scaling relation for  $D_{\parallel}(L, t)$  can be written as

$$D_{\parallel}(L, t) = L f_{\parallel}(L/t^{1/z}) \approx \begin{cases} t^{1/z} & \text{if } 1 \ll t \ll L^z, \\ L & \text{if } t \gg L^z. \end{cases} \quad (8)$$

A similar relation to the case for  $1 \ll t \ll L^z$  in Eq. (8) was also suggested in Ref. [12]. The relation for  $t \gg L^z$  in Eq. (8) is new and physically means that damages spread throughout the sample in the saturation regime (or  $t \gg L^z$ ), so that DSs in the saturation regime can show the self-affinity of the surface growth as  $\bar{d}_{\perp}(d_{\parallel}, t = \infty) = L^{\alpha}$  and  $D_{\perp}(L, t = \infty) = L^{\alpha}$ . From Eq. (6) and Eq. (8) one can expect that the scaling relation

$$P(d_{\parallel}, t) = d_{\parallel}^{-1} f_p(d_{\parallel}/t^{1/z}) \quad (9)$$

holds, where  $f_p(0) = \text{const}$  or  $P(d_{\parallel}, t \gg L^z) \approx d_{\parallel}^{-1}$ . From Eqs. (4), (7), and (9) we also get

$$D_{\perp}(L, t) \approx \begin{cases} t^{\beta} & \text{if } 1 \ll t \ll L^z, \\ L^{\alpha} & \text{if } t \gg L^z. \end{cases} \quad (10)$$

To confirm the suggested scaling *Ansätze* (4), (8), (9), and (10) we study DSs in the various surface growth models by simulations. Surface growth models which satisfy the dynamical scaling law (1) can be categorized into two large classes. One class consists of normal roughening models in which the exponent  $\alpha$  satisfies  $\alpha < 1$ . The famous models which belong to this class are the Family model [14], restricted solid-on-solid (RSOS) model [19], etc. The other class consists of the superroughening models in which  $\alpha$  satisfies  $\alpha > 1$ . The famous models which belong to the second class are the Das Sarma–Tamborenea (DT) model [17], large curvature (LC) model [20], etc.

### III. SIMULATION RESULTS FOR NORMAL ROUGHENING MODELS

Our simulation is done in the substrate dimension  $d = 1$ . In this section we explain the simulation data for DSs in the class of the normal roughening models. Here we mainly report the data of DSs in the RSOS model. However, we have confirmed that the main results hold nearly in the same way for the other models such as Family model.

Figure 1 shows the data of the RSOS model for  $\bar{d}_{\perp}(d_{\parallel}, t)$  versus  $t$  when  $L = 1024$  and  $t \ll L^z$ . First note the data in the inset of Fig. 1, which is for  $\bar{d}_{\perp}(d_{\parallel} = 8, t)$ . The behavior of data in the inset is common for different  $\bar{d}_{\perp}(d_{\parallel}, t)$ 's. The common behavior is as what follows. For  $t < t_i(d_{\parallel})$  there is no damage in the column at  $d_{\parallel}$ . Around  $t_i$ , damages begin to appear and furthermore the initial transient regime with the spike-type data appears. After the initial transient regime around  $t_i$ , the data follow the second case of Eq. (4),

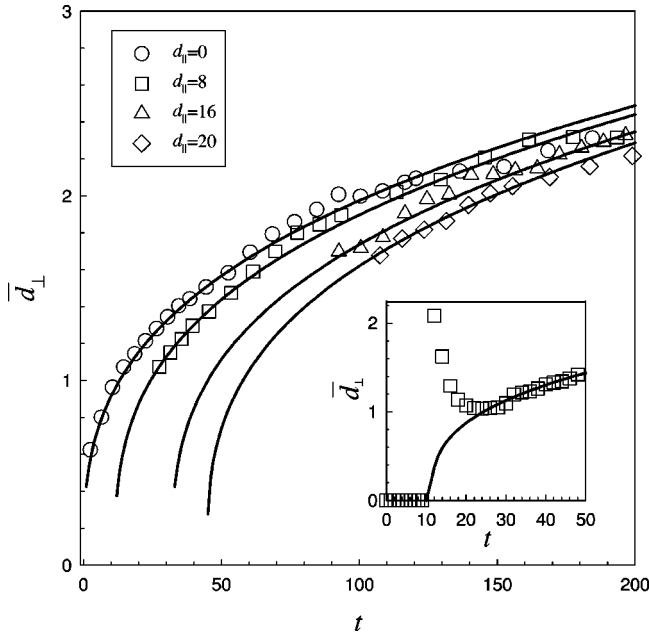


FIG. 1. Data for the time dependence of  $\bar{d}_\perp$  at different  $d_\parallel$ 's in the RSOS model. The inset is the data of  $\bar{d}_\perp$  at  $d_\parallel=8$  with initial spike-type data. The data in the main part of the figure are shown with omitting the initial spike-type data. The solid curves represent  $\bar{d}_\perp(d_\parallel, t) = A(t - cd_\parallel^z)^\beta$  with  $z = 1.53$  and  $\beta = 0.32$ .

$\bar{d}_\perp(d_\parallel, t) = A(t - cd_\parallel^z)^\beta$ , well. The initial transient regime should be from the unmaturing correlation between the just-born damages around  $d_\parallel$  and the already existing damages. The data for different  $d_\parallel$ 's in the main part of Fig. 1 are presented without showing the data of the initial transient regime around  $t_i(d_\parallel)$  for simplicity. The curves shown in Fig. 1 are obtained in the following way. First, using the data for  $\bar{d}_\perp(d_\parallel=0, t)$  and the relation  $\bar{d}_\perp(d_\parallel=0, t) = At^\beta$ , we have obtained  $A = 0.43$  and  $\beta = 0.32$ , where the exact value of  $\beta$  of the RSOS model is  $1/3$ . Next from the data for  $t_i(d_\parallel)$  for various  $d_\parallel$ 's and the relation  $t_i(d_\parallel) = cd_\parallel^z$ ,  $c = 0.50$ , and  $z = 1.53$  have been obtained. Using these independently obtained values for  $\beta$ ,  $z$ ,  $A$ , and  $c$  and the function  $\bar{d}_\perp(d_\parallel, t) = A(t - cd_\parallel^z)^\beta$  the curves in Fig. 1 are drawn. These curves fit the data for the various  $\bar{d}_\perp$ 's well except for the transient regime. In Fig. 2 the data of  $\bar{d}_\perp$  for various  $d_\parallel$ 's are shown to collapse onto a single curve using the function  $\bar{d}_\perp(d_\parallel, t) = Ax^\beta$  with  $x = t - cd_\parallel^z$ . Of course the data of the initial transient regimes are not included in Fig. 2. From Figs. 1 and 2 we can conclude that DS in the RSOS model satisfies the first and second cases of Eq. (4) quite well. Figure 3 shows the data of  $\bar{d}_\perp(d_\parallel, t=\infty)$  for various  $d_\parallel$ 's. The substrate sizes used are  $L = 128, 256, 512, 1024$ . The data for the various  $d_\parallel$ 's with the same  $L$  have the same value. The data in Fig. 3 have been fitted to the third case of Eq. (4),  $\bar{d}_\perp(d_\parallel, t=\infty) \approx L^\alpha$ , and the obtained  $\alpha$  is  $\alpha = 0.51$ , which is very close to the exact value  $\alpha = 1/2$  of the RSOS model. The result in Fig. 3 shows that DS in the RSOS model satisfies the third case of Eq. (4) well. Thus from the results in Figs. 1, 2, and 3 DS in the RSOS model satisfies the dynamical self-affinity described by Eq. (4) quite well and the obtained

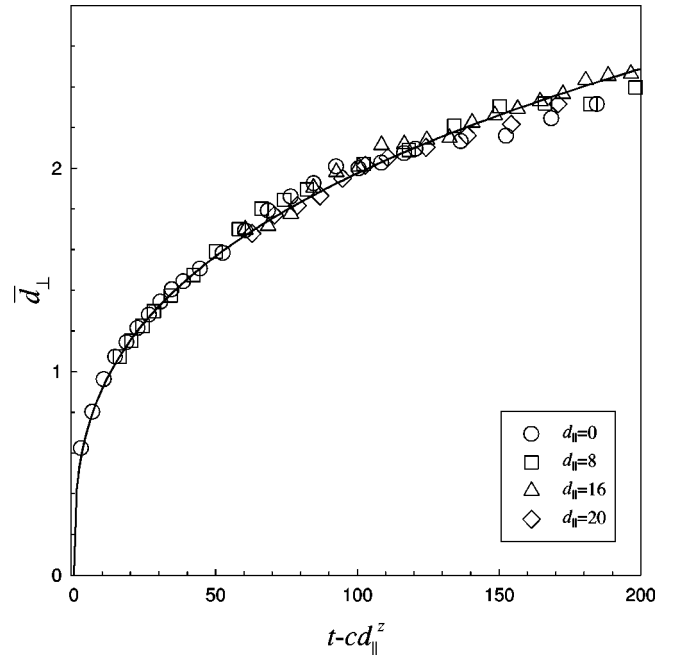


FIG. 2. The collapse of the data in Fig. 1 onto a single curve  $\bar{d}_\perp = Ax^\beta$  with  $x = t - cd_\parallel^z$ .

values of the exponents  $\alpha$ ,  $\beta$ , and  $z$  agree well with the exactly known values.

Next we want to discuss the simulation results of the RSOS model for  $P(d_\parallel, t)$  and  $D_\parallel(L, t)$ . The inset of Fig. 4 shows the data for  $P(d_\parallel, t)$  at several different  $t$ 's. The data have been taken by averaging over 3000 independent runs using the substrate with  $L = 1024$ . As one can see in Fig. 4,

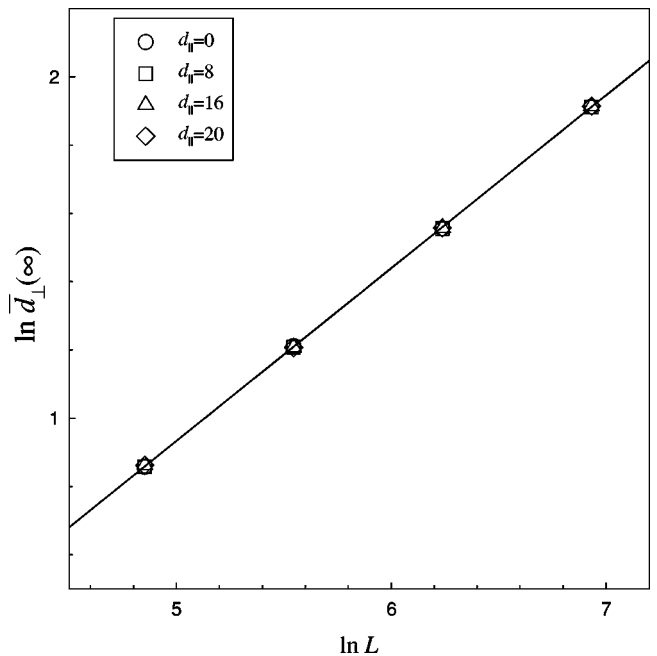


FIG. 3. In-ln plot of  $\bar{d}_\perp$  in the saturation regime (or  $t = \infty$ ) against  $L$  for the RSOS model. The substrate sizes used are  $L = 128, 256, 512, 1024$ . Note that the data for different  $d_\parallel$ 's have the same value. The solid line represents  $\bar{d}_\perp(d_\parallel, t = \infty) = L^\alpha$  with  $\alpha = 0.51$ .

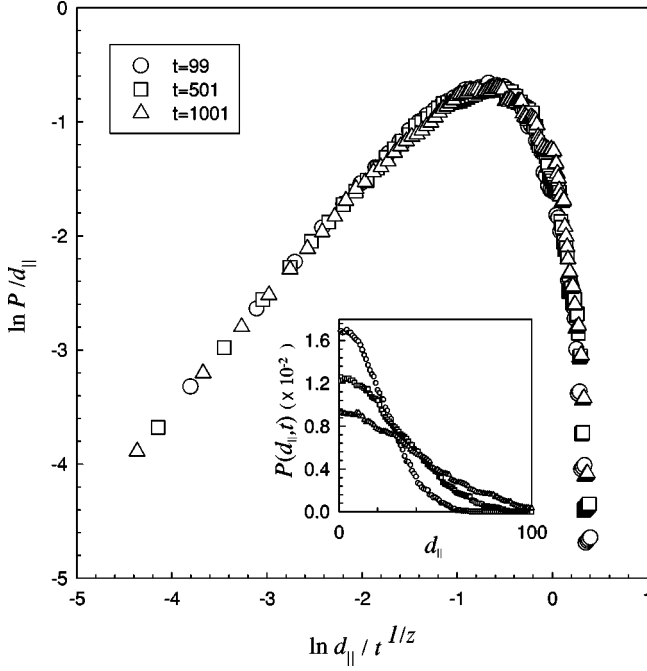


FIG. 4. The data in the RSOS model for  $P(d_{\parallel}, t)$  at various  $t$ 's are shown to collapse onto a single curve using the function  $P(d_{\parallel}, t) = d_{\parallel}^{-1} f_p(d_{\parallel}/t^{1/2})$  with  $z=3/2$ . Inset shows the data for  $P(d_{\parallel}, t)$  at various  $t$ 's.

the data for  $P(d_{\parallel}, t)$  for various  $t$ 's collapse well onto a single curve using the function  $P(d_{\parallel}, t) = d_{\parallel}^{-1} f_p(d_{\parallel}/t^{1/2})$ . The value of  $z$  used for the collapse diagram in Fig. 4 is  $3/2$ , which is the exactly known value for the RSOS model. From the results in Fig. 4 it can be seen that  $P(d_{\parallel}, t)$  of the RSOS model satisfies the scaling law (9) well. We have also confirmed that  $P(d_{\parallel}, t)$  for other normal roughening models such as the Family model satisfies Eq. (9) well. Figure 5 shows the data of the RSOS model for  $D_{\parallel}(L, t)$ . The data in the inset of Fig. 5 have been obtained from the simulation for  $t \leq L^z$  on the substrate with  $L=1024$ . From the  $\ln D_{\parallel} - \ln t$  plot for the data in the inset of Fig. 5 and Eq. (8) for  $t \leq L^z$ ,  $1/z = 0.66$  is obtained. This result is consistent with Eq. (8) for  $t \leq L^z$ , because the exact value of  $z$  in the RSOS model is  $3/2$ . The data in the main part of Fig. 5 are those for  $D_{\parallel}$  when  $t \geq L^z$ . The substrate sizes used are  $L=128, 256, 512, 1024$ . The slope of the  $\ln D_{\parallel} - \ln L$  plot in Fig. 5 is nearly the same as 1 and this result is also consistent with  $D_{\parallel} \approx L$  for  $t \geq L^z$ . The simulation results of the RSOS model for  $D_{\parallel}$  both in the inset of Fig. 5 and in the main part of Fig. 5 satisfy Eq. (8) rather well. We have also confirmed that  $D_{\parallel}(L, t)$  for other normal roughening models such as the Family model satisfies Eq. (8) well. We have also confirmed that Eq. (10) holds for normal roughening models by simulations. The validity of Eq. (10) can easily be seen from the data in Figs. 1 and 3.

#### IV. SIMULATION RESULTS FOR SUPERROUGHENING MODELS

We next explain the simulation data for DSs in the class of the superroughening models. Here we mainly report the data of DSs in DT model. It is found that the velocity of initial lateral DS in the DT model is very rapid compared to

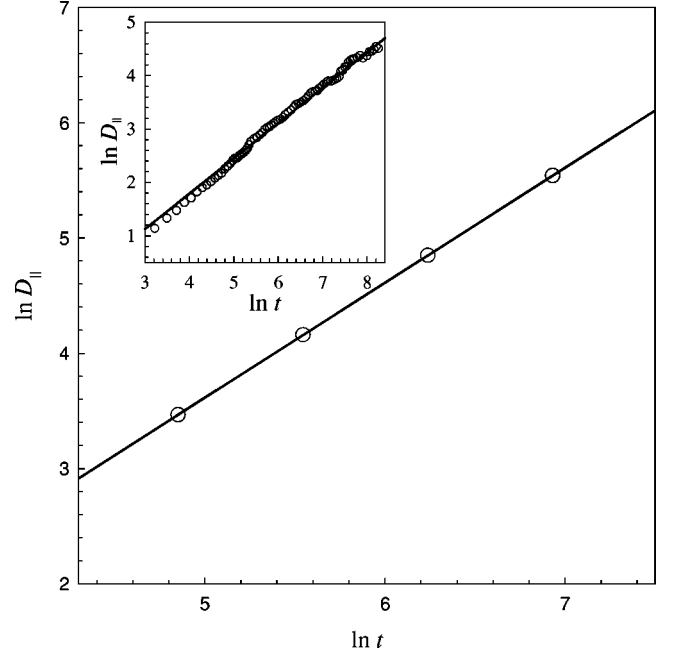


FIG. 5.  $\ln\text{-}\ln$  plot of  $D_{\parallel}(L, t)$  against  $L$  in the saturation regime (or when  $t=\infty$ ) for the RSOS model. The substrate sizes used are  $L=128, 256, 512, 1024$ . The solid line represents  $D_{\parallel}(L, t=\infty) \approx L$ . The inset shows the  $\ln\text{-}\ln$  plot of  $D_{\parallel}(L, t)$  versus  $t$  for  $t \leq L^z$  and  $L=1024$ . The solid line in the inset represents  $D_{\parallel}(L, t) \approx t^{1/2}$  with  $1/z=0.66$ .

that in normal roughening models. From the data for  $t_i(d_{\parallel})$  for various  $d_{\parallel}$ 's and the relation  $t_i(d_{\parallel}) = c d_{\parallel}^z$ , the obtained  $c$  value in the DT model is anomalously small or  $c \leq 0.0001$ . This result means that the initial lateral DS occurs more rapidly than expected [or  $t_i(d_{\parallel}) \ll d_{\parallel}^z$ ]. We have also found anomalously rapid DS in the LC model. Similar anomalous behavior in the LC model was found in a somewhat different sense in Ref. [12]. We thus believe that the anomalously rapid lateral spreading of the initial damages is common in the class of superroughening models. Even though there should exist anomalously rapid DS initially, DS in the DT model has been confirmed to satisfy the dynamical self-affinity or Eq. (4). Figure 6 shows that the data of  $\bar{d}_{\perp}$  for various  $d_{\parallel}$ 's in the DT model collapse rather well into a single curve using the function  $\bar{d}_{\perp}(d_{\parallel}, t) = A x^{\beta}$  with  $x = t - c d_{\parallel}^z$ . The used data in Fig. 6 are of course those in the regime  $1 \ll t - c d_{\parallel}^z \ll L^z$ . The obtained  $\beta$  value from Fig. 6 is 0.37, which is very close to the exactly known value  $\beta = 3/8$  of the DT model. The inset of Fig. 6 shows the data of  $\bar{d}_{\perp}(d_{\parallel}, t=\infty)$  for various  $d_{\parallel}$ 's in the DT model. The substrate sizes used are  $L=32, 64, 128, 256$ . The data in the inset for the various  $d_{\parallel}$ 's with the same  $L$  have the same value as in the RSOS model. The data in the inset have also been fitted to  $\bar{d}_{\perp}(d_{\parallel}, t=\infty) \approx L^{\alpha}$  and the obtained  $\alpha$  value is 1.53, which is very close to the exact value  $\alpha = 3/2$  of DT model. From Fig. 6 it can also be concluded that DS in the DT model satisfies the dynamical self-affinities described by Eq. (4) well and the obtained values of  $\alpha$  and  $\beta$  from Eq. (4) agree well with the known values of the corresponding model. We have also confirmed that DS in other superroughening models such as the LC model satisfies Eq. (4) well.

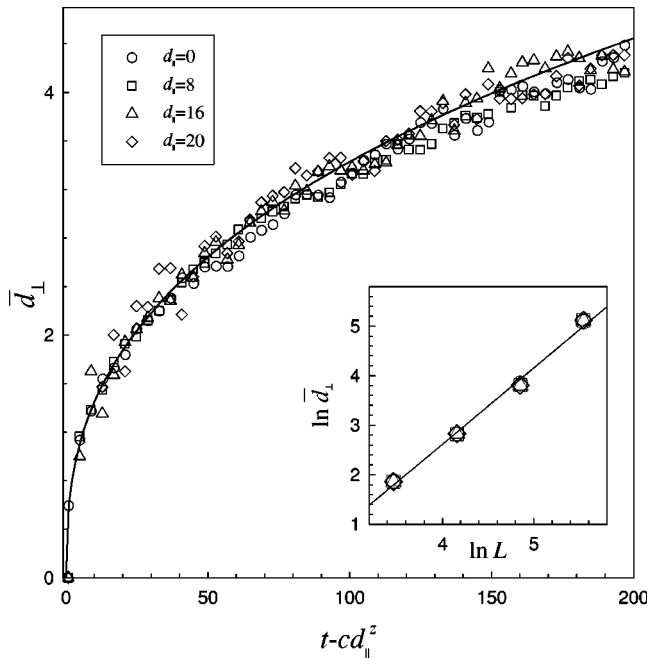


FIG. 6. The collapse of the data for  $\bar{d}_\perp(d_\parallel, t)$  in the DT model onto a single curve  $\bar{d}_\perp = Ax^\beta$  with  $x = t - cd_\parallel^z$  when  $x \ll L^z$ . The  $\beta$  and  $z$  values used are 0.37 and 4.1, respectively. The inset shows the ln-ln plot of  $\bar{d}$  in the saturation regime (or  $t = \infty$ ) versus  $L$  for the DT model. The substrate sizes used are  $L = 32, 64, 128, 256$ . The solid line in the inset represents  $\bar{d}(d_\parallel, t = \infty) = L^\alpha$  with  $\alpha = 1.53$ .

Next we want to discuss the simulation results of superroughening models for  $P(d_\parallel, t)$  and  $D_\parallel(L, t)$ . In the superroughening model, especially in the DT and LC models, it has been found that the data for  $P(d_\parallel, t)$  when  $t \ll L^z$  do not satisfy Eq. (9) well. This result can be expected from the anomalously rapid damage spreading in the initial stage of growth, which we have mentioned previously. Instead  $P(d_\parallel, t)$  has been found to satisfy  $P(d_\parallel, t) = d_\parallel^{-\kappa} f_p(d_\parallel/t^{1/z})$  with  $0 < \kappa < 1$  when  $t \ll L^z$ . This anomalous behavior in the DT and LC models may come from the fact that the damaged sites do not form one connected cluster, but form several different clusters [12]. In contrast it has been confirmed that  $P(d_\parallel, t) \approx d_\parallel^{-1}$  when  $t \gg L^z$ , which is

consistent with Eq. (9) when  $t \gg L^z$ . From the simulation results of superroughening models for  $P(d_\parallel, t)$  we can expect that  $D_\parallel$  when  $t \ll L^z$  does not satisfy Eq. (8) when  $t \ll L^z$ , but  $D_\parallel$  for  $t \gg L^z$  satisfies  $D_\parallel(L, t \rightarrow \infty) \approx L$  well. We have confirmed  $D_\parallel(L, t \rightarrow \infty) \approx L$  for superroughening models by simulations.

## V. SUMMARY AND DISCUSSION

We have shown that DS in surface growth models satisfies the dynamical self-affinity [Eq. (4)] quite well as can be seen from Figs. 1, 2, 3, and 6. From this result it has also been concluded that one can obtain the exponents  $\alpha$ ,  $\beta$ , and  $z$  by using the simple scaling relation  $\bar{d}_\perp(d_\parallel=0, t) = L^\alpha f_\perp(t/L^z)$ , i.e., the relation for the vertical DS distance of the column at which the initial damage is assigned.

For normal roughening models such as the RSOS model and Family model  $P(d_\parallel, t)$  and  $D_\parallel(L, t)$  satisfy the scaling *Ansätze* (9) and (8) quite well. This result physically means that we can understand the critical behavior of the correlation length  $\xi(L, t)$  of normal roughening models directly by studying  $P(d_\parallel, t)$  and  $D_\parallel(L, t)$ . In contrast damages in superroughening models initially spread with anomalously rapid velocity and  $P(d_\parallel, t)$  and  $D_\parallel(L, t)$  do not follow Eqs. (9) and (8) initially (or for  $t \ll L^z$ ). This result may come from the fact that in the LC and DT models the growth mechanisms depend on the height configurations of the next nearest neighbors of the randomly chosen column as well as the nearest neighbors of it. However, in both normal roughening models and superroughening models we have confirmed that the relations  $P(d_\parallel, t) \approx d_\parallel^{-1}$  and  $D_\parallel(L, t) \approx L$  hold in the saturation regime (or for  $t \gg L^z$ ). This result physically means that damages are not frozen in some local area but spread throughout the sample in the saturation regime. This sample-size spreading guarantees that the self-affine properties of the surface roughenings can also be studied by DS concepts.

## ACKNOWLEDGMENTS

This work was supported in part by the Korean Science and Engineering Foundation (Grant No. 98-0702-05-01-3) and by the Brain Korea 21 project.

[1] P. Grassberger, *Physica A* **214**, 547 (1995).  
 [2] S. A. Kauffman, *J. Theor. Biol.* **22**, 437 (1969).  
 [3] N. Jan and L. de Arcangelis, *Annu. Rev. Comput. Phys.* **1**, 1 (1994).  
 [4] H. Hinrichsen and E. Domany, *Phys. Rev. E* **56**, 94 (1997).  
 [5] H. E. Stanley, D. Stauffer, J. Kertesz, and H. J. Herrmann, *Phys. Rev. Lett.* **59**, 2326 (1987).  
 [6] H. Hinrichsen, E. Domany, and D. Stauffer, *J. Stat. Phys.* **91**, 807 (1998).  
 [7] P. Grassberger, *J. Stat. Phys.* **79**, 13 (1995).  
 [8] P. Grassberger, *J. Phys. A* **22**, L1103 (1989); H. Hinrichsen, *Phys. Rev. E* **55**, 219 (1997).  
 [9] T. Vojta and M. Schreiber, *Phys. Rev. E* **58**, 7998 (1998).  
 [10] F. D. Nobre, A. M. Mariz, and E. S. Sousa, *Phys. Rev. Lett.* **69**, 13 (1992).

[11] B. Derrida and G. Weisbuch, *Europhys. Lett.* **4**, 657 (1987).  
 [12] J. M. Kim, Y. Lee, and I. Kim, *Phys. Rev. E* **54**, 4603 (1996).  
 [13] J. Krug and H. Spohn, in *Solids Far From Equilibrium: Growth, Morphology and Defects*, edited by C. Godreche (Cambridge University Press, New York, 1991); *Dynamics of Fractal Surfaces*, edited by F. Family and T. Vicsek (World Scientific, Singapore, 1991); A.-L. Barabási and H. E. Stanley, *Fractal Concepts in Surface Growth* (Cambridge University Press, Cambridge, England, 1995); T. Halpin-Healy and Y. -C. Zhang, *Phys. Rep.* **254**, 215 (1995); J. Krug, *Adv. Phys.* **46**, 139 (1997).  
 [14] F. Family, *J. Phys. A* **19**, L441 (1986).  
 [15] S. F. Edwards and D. R. Wilkinson, *Proc. R. Soc. London, Ser. A* **381**, 17 (1982).  
 [16] D. E. Wolf and J. Villain, *Europhys. Lett.* **13**, 389 (1990).

- [17] S. Das Sarma and P. Tamborenea, Phys. Rev. Lett. **66**, 325 (1991).
- [18] C. Herring, J. Appl. Phys. **21**, 301 (1950); W. W. Mullins, *ibid.* **28**, 333 (1957); **30**, 77 (1959).
- [19] J. M. Kim and J. M. Kosterlitz, Phys. Rev. Lett. **62**, 2289 (1989); J. M. Kim, J. M. Kosterlitz, and T. Ala-Nissila, J. Phys. A **24**, 5569 (1991).
- [20] J. M. Kim and S. Das Sarma, Phys. Rev. Lett. **72**, 2903 (1994).
- [21] S. H. Yook, J. M. Kim, and Yup Kim, Phys. Rev. E **56**, 4085 (1997).